

# Optimally Discriminant Moments for Speckle Detection in Real B-Scan Images

Robert Martí<sup>1</sup>, Joan Martí<sup>1</sup>, Jordi Freixenet<sup>1</sup>, Joan Carles Vilanova<sup>2</sup>,  
and Joaquim Barceló<sup>2</sup>

<sup>1</sup> Computer Vision and Robotics Group. University of Girona, Spain  
{marly, joanm, jordif}@eia.udg.es

<sup>2</sup> Girona Magnetic Resonance Center. Girona, Spain  
{kvilanova, rmgirona}@comg.es

**Abstract.** Detection of speckle in ultrasound (US) images has been regarded as an important research topic in US imaging, mainly focusing on two specific applications: improving signal to noise ratio by removing speckle noise and, secondly, for detecting speckle patches in order to perform a 3D reconstruction based on speckle decorrelation measures.

A novel speckle detection proposal is presented here showing that detection can be improved based on finding optimally discriminant low order speckle statistics. We describe a fully automatic method for speckle detection and propose and validate a framework to be efficiently applied to real B-scan data, not being published to date. Quantitative and qualitative results are provided, both for real and simulated data.

## 1 Background

US imaging captures the difference of sound scattering and reflection in tissues. Taking into account spatially randomly distributed sub-resolution scatterers, one can talk about incoherent scattering which gives rise to **speckle noise** or fully developed speckle. However, if this distribution follows a given pattern, a **coherent** component is introduced. The main aim of this work is to provide an automatic method for the detection of fully developed speckle patterns in B-scans. A common approach is to describe speckle using a known statistical model. Various models have been proposed for speckle characterisation, Rayleigh and Rician models were originally used but more general models such as the Nakagami [1],  $K$  [2], Generalised  $K$  and Homodyned  $K$  distributions [3,4] have shown to account for better speckle description at the expense of a more complex formulation. An alternative approach, adopted here, is to describe speckle based on statistical features extracted from the amplitude moments of the B-scan. The work presented here is based on an earlier work [5] but incorporates relevant novel aspects such as the optimally discriminant computation of speckle statistics and the methodology for its fully automatic application to real B-scan data. The paper is structured as follows: Sect. 2 presents the formulation for obtaining optimally discriminant speckle statistics; Section 3 proposes a method for speckle detection in B-scans, while Sect. 4 shows evaluation results using simulated and real data. The paper finishes with conclusions and future work.

## 2 Speckle Characterisation

Speckle in ultrasound images is commonly characterised by three parameters: the coherent signal energy  $s^2$ , the diffuse signal energy  $2 * \sigma^2$  and the number of scatters per resolution cell  $\mu$ . The coherent and diffuse signals are also commonly expressed as the ratio  $k = s/\sigma$ , the proportion of coherent to diffuse signal. As demonstrated by different authors [5,6], speckle can be characterised by two low order moments: the ratio between the mean and the standard deviation ( $R$ ) and the skewness ( $S$ ), defined as follows,

$$R = \frac{E\{A^v\}}{\sqrt{E\{A^{2v}\} - E^2\{A^v\}}} \quad S = \frac{E\{(A^v - E\{A^v\})^3\}}{(E\{A^{2v}\} - E^2\{A^v\})^{3/2}} \quad (1)$$

where  $A$  is the signal amplitude, and  $v$  the power of the statistical moment. Effectively,  $R$  and  $S$  can be computed using  $v$  values different from one. This issue is important as the use of an specific value of  $v$  could lead to a better discrimination between speckle and non-speckle signals. For instance, in all experiments described by Prager et al. [5] a fixed  $v$  value was used ( $v = 1.8$  for simulated and  $v = 1$  for real US images). As noted in [7], this assertion may not be always valid. Authors show that an analysis of the discriminant power of the  $R$ - $S$  features should be carried out in order to determine the optimal order of the statistics. Nevertheless, their experiments are based on simulated data and do not discuss how this optimal  $v$  value affects the final speckle detection algorithm, nor how this criteria can be applied to real B-scan data.

### 2.1 Discriminant Power Analysis

The  $R$ - $S$  statistics can be regarded as features for a classic pattern recognition problem [8]: given a set of feature values classify them as being speckle or non-speckle. As a set of  $R$ - $S$  is obtained for each sampled  $v$  value, one could think that the most appropriate  $R$ - $S$  features are those which maximise a certain measure of discriminating power. One of the most commonly used methods is the analysis of the *within class* ( $S_w$ ) and the *between class* ( $S_b$ ) scatter matrices [8]. Defining the matrix  $S_m$  as the sum of the  $S_w$  and  $S_b$ , different measures of discrimination power can be computed. In order to follow a consistent notation with [7], those measures are referred to as  $J_1$ ,  $J_2$  and  $J_3$  and are defined as follows.

$$J_1 = trace(S_m)/trace(S_w) \quad J_2 = det(S_m)/det(S_w) \quad J_3 = trace(S_w^{-1} * S_b) \quad (2)$$

For all cases a higher value denotes higher class separability, although this criteria does not always coincide for all measures, which, excerpted from the experiments, is specially true for  $J_1$  measures. Back to the problem of speckle detection, having those measures of class separability one can conduct different experiments in order to obtain the value of  $v$  which maximises class separability, we will refer to this value as  $v_{opt}$ . Nevertheless, the problem of developing a method for detecting speckle in real B-scan images using those discriminant features has not been addressed yet. This is presented in the next section.

### 3 Speckle Detection in Real B-Scans

This section adapts the speckle detection methodology in order to be applied to real B-scan ultrasound images. An added difficulty is that intensity data in B-scan images is log compressed by the ultrasound machine in order to account for the full dynamic range. If the original non-compressed signal is unavailable, intensity information needs to be decompressed in order to correctly characterise speckle. Several authors suggest a compression of the form  $p = D \ln(I) + G$ , where  $p$  is the final B-scan intensity,  $D$  the compression factor,  $G$  an offset value and  $I$  the original intensity signal. The offset value is often disregarded as it does not affect the statistics of the speckle. It is then  $D$  the important factor to be determined in order to obtain a good speckle detection.

#### 3.1 Speckle Detection

As previously stated, our work builds up on the speckle detection methodology proposed by Prager et al. [5], but incorporates novel aspects such as the optimal selection of the statistics applied to real B-scans and removing the need of manual intervention, aspects which we believe make the method more robust. Prager et al. proposal is based on a simultaneous method for estimating B-scan decompression parameters and subsequently detect speckle regions based on the ellipsoid discriminant function obtained from simulated speckle data. The ellipsoid function is used to classify a patch as being speckle if its  $R - S$  features lie within the ellipse. The original approach presents some drawbacks. A first issue is the need of manually detecting initial speckle regions in order to extract sample statistics, prone to errors due to human variability and to the fact that in some images it is difficult to obtain those regions. Manual intervention is also needed in order to obtain the ellipse parameters for the speckle discriminant function. This is solved in this work by using eigenanalysis of the covariance matrix obtained from the R-S simulated data. Another important drawback is the fact that  $R - S$  features are computed using an arbitrarily value. The power of the statistics can play an important role in discriminating speckle regions as it is shown in the results section. The steps of our proposal are described below,

1. Obtain an **ellipse discriminant function** from speckle simulated data for different  $v$  values ranging from 0 to 3 (i.e. with increments of 0.1).
2. Automatically detect **core speckle** and **core non-speckle** regions and estimate decompression factor  $D_v$  from the real B-scan data (see Sect. 3.2).
3. Using speckle and non-speckle, compute  $R - S$  statistics and find  $v_{opt}$ , the  $v$  value where those statistics are optimally discriminant.
4. Adapt the ellipse centre parameters using the mean  $R - S$  features from the speckle patches, similarly to the original method.
5. For all patches in the image, decompress it using the  $D_{v_{opt}}$  value, obtain  $R - S$  features and use the ellipse discriminant function to assert if it is a speckle patch (is inside the ellipse), also similarly to the original method.

The following section describes the core speckle and decompression estimation method (step 2 of the proposal).

### 3.2 Core Speckle and Decompression Estimation

In order to estimate the decompression factor, a number of speckle patches needs to be detected. However, speckle patches can not be detected if no decompression estimation is obtained. This is clearly an optimisation problem where decompression and speckle patches need to be simultaneously estimated. In the original work [5] this was approached by manually detecting fully developed speckle patches. Here, this is solved using a RANSAC based approach, which automatically detects representative speckle and non-speckle patches from randomly sampled patches in the B-scan data.

The detection of speckle and non-speckle patches is based on the assumption that the estimated decompression values  $D$  found after an optimisation process (see [5]) are stable as a function of  $v$  for speckle patches. In the case of non-speckle patches those values will present high variability for different  $v$  values, explained by the fact that optimisation will be unable to find a meaningful  $D$  value. This assumption is corroborated by different experiments on both simulated and real data, some of them shown in Sect. 4.2. The method for core speckle and simultaneous decompression estimation is described using the following steps:

1. Choose an initial compression value  $D$ .
2. Extract a  $N$  random patches from the B-scan data.
3. For each patch  $p$ 
  - (a) **Decompress** the patch intensity using  $I_p = exp(p/D)$
  - (b) Compute  $R - S$  from  $I_p$ , for a range of  $v$  values from 0 to 3, ( $F_{pv}$ ).
  - (c) For each  $F_{pv}$  use an optimisation algorithm to estimate the decompression value,  $D_{pv}$ .
4. Extract the most stable (smallest standard deviation)  $D_{pv}$  values as a function of  $v$ ,  $D'_{pv}$ .
5. Compute the median of the  $D'_{pv}$  obtaining a final estimation of the compression factor as a function of  $v$ ,  $D_v$  (see Sect. 4.2).
6. Core **speckle** patches are defined as the  $N_{sp}$  patches with  $D_{pv}$  values closest to  $D_v$ , while core **non-speckle** patches will be randomly sampled ( $N_{nsp}$ ) from the patches with the largest difference to  $D_v$ .

In addition to the log compressed image, some modern ultrasound machines already provide the uncompressed echo amplitude signal. In that case, the method would not need to estimate the decompression parameter, making the core speckle and non-speckle step less computationally costly, avoiding the use of the optimisation algorithm in order to obtain the estimation of the decompression factor  $D$ . However, if this information is unavailable, for instance due to the limitations of the ultrasound scanner or to the fact that images are from retrospective studies (where non-compressed images are not available), the presented method provides an estimation of this compression.

## 4 Evaluation and Results

### 4.1 Discriminant Analysis

Other works have already justified the need of finding discriminant statistics for speckle detection [7]. Nevertheless this needs to be investigated as a different detection approach is adopted here and moreover, the discriminant analysis applied to real B-scan data conforms one of the novel aspects of our approach.

As an initial evaluation, different experiments are presented using simulated data. A total of four different speckle and non-speckle patterns have been simulated using different  $k$  and  $\mu$  parameters, namely  $I_a = (0, 50)$  as fully developed speckle and  $I_b = (1, 50)$ ,  $I_c = (0, 2)$ ,  $I_d = (1, 2)$  as non-speckle patterns. For each pattern a total of 1000 different sets of 1000 samples have been simulated, subsequently  $R - S$  features have been computed as a function of  $v$ . Fig. 1(a) shows class separability for the 2-class problem as a function of  $v$ . The maximum value for  $J_1$  is around 1.3, whereas  $J_2$  and  $J_3$  seem slightly consistent in finding the  $v_{opt} = 0.9$ . As pointed out previously  $J_2$  and  $J_3$  values correspond to similar discrimination criteria. Therefore, and similarly to [7],  $J_3$  will be used as discriminant criteria ( $J_2$  could also be used). Those results, and other simulated experiments not shown here, suggest that class separability is not close to a fixed value as suggested in [5]. For the  $v_{opt}$  value, Fig. 1(b) shows the scatter plot of the  $R$ - $S$  features where a clear discrimination can be seen between the data except for  $I_a$  and  $I_b$ . This overlap is explained by the similar parameters used, related to fully developed speckle and speckle with an small amount of coherent scattering.

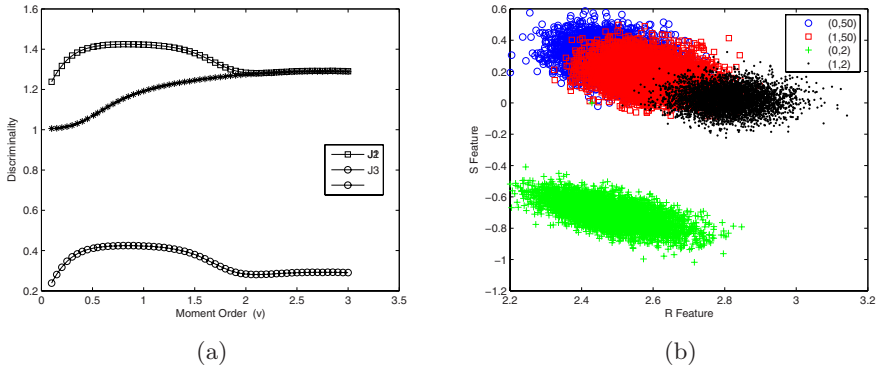


**Fig. 1.** 2-class problem: (a) Class separability as a function of  $v$  and (b) the scatter plot of the  $R$ - $S$  features for the case where  $J_3$  is maximal ( $v_{opt} = 0.9$ )

Another experiment is presented in order to asses if the use of the discriminant criteria for  $v$  value corresponds to a better speckle detection rate. Speckle and non-speckle data characterised by different parameters has been simulated.

An ellipsoid discriminant function has been fitted using the  $R - S$  features from speckle data for different  $v$  values. The experiment is based on selecting a number of random samples from the simulated data and test if they belong to speckle using the ellipsoid function. The aim is to evaluate if the optimally discriminant  $v$  value ( $v_{opt}$ ) improves speckle detection results. Table 1 summarises the results in two different simulations (600 and 4000 sample sizes) in terms of correct classification rate ( $CCR$ ), sensitivity ( $Sens$ ) and specificity ( $Spec$ ). For the experiment with 4000 samples, sensitivity and  $CCR$  using  $v_{opt}$  are increased, while specificity does not significantly change compared to other  $v$  values. When a smaller number of data is used, this difference is not that significant, although the  $v_{opt}$  does not degrade the results and is in line with the best detection rates. Results with different simulated data (not included here) also corroborates those findings. In conclusion, the use of  $v_{opt}$  obtains the optimal  $v$  statistic for speckle detection in our approach.

**Table 1.** Speckle detection for simulated data using different sample sizes: 600 (left) and 4000 (right) samples. For both tables the last row corresponds to the  $v_{opt}$  value.

v	CCR	Sens	Spec	v	CCR	Sens	Spec
3	0.844	0.975	0.676	3	0.893	0.983	0.779
2	0.853	0.969	0.704	2	0.895	0.981	0.785
1.8	0.846	0.979	0.678	1.8	0.891	0.980	0.778
1.1	0.852	0.980	0.685	1.2	0.900	0.991	0.783

### 4.2 Decompression Estimation

The assumption that the decompression values found after optimisation are stable as a function of  $v$  for speckle patches, compared to non-speckle patches is evaluated. A set of speckle and non-speckle patches have been manually labeled, subsequently, step 3 described in Sect. 3.2 is applied in order to obtain the behaviour of a  $D$  estimation for both speckle and non-speckle patches as a function of  $v$ . Figure 2(a) shows these estimations for speckle and non-speckle, it is clear that non-speckle regions obtain a highly variable  $D$  estimation, whereas speckle patches are fairly stable. In our method, a decompression estimation as a function of the  $v$  values is obtained by computing the median of these stable values. This estimation,  $D_v$ , is shown in Fig. 2(b).

### 4.3 Detection of Core Speckle and Non-speckle

Figure 3 shows the core speckle and non-speckle detection results using the described approach in real B-scan data from a prostatic phantom. The  $N_{sp}$  and  $N_{nsp}$  values are set to 20, a non particularly critical value. Core speckle clearly shows typical low intensity fully developed speckle patches, whereas core non-speckle are characterised by the high contrast regions with important coherent signal components.

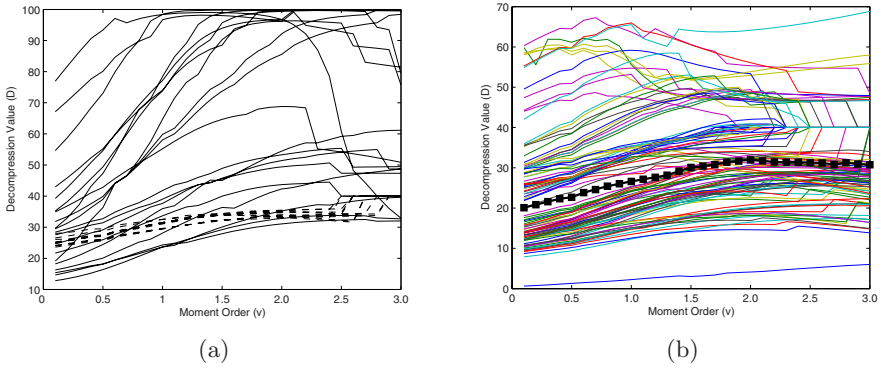


**Fig. 2.** Decompression estimation: (a)  $D$  estimation as a function of  $v$  using manually labeled speckle (dotted) and non-speckle (solid) patches; (b) final  $D_v$  estimation from the median of the most stable estimations

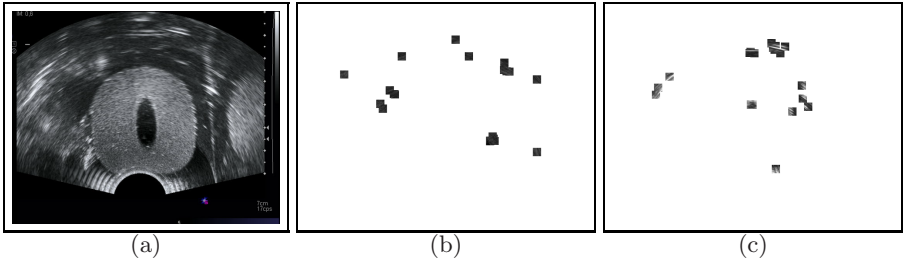


**Fig. 3.** Results for the proposed core speckle detection in prostatic phantom images. (a) original B-scan, (b) core speckle, (c) core non-speckle patches.

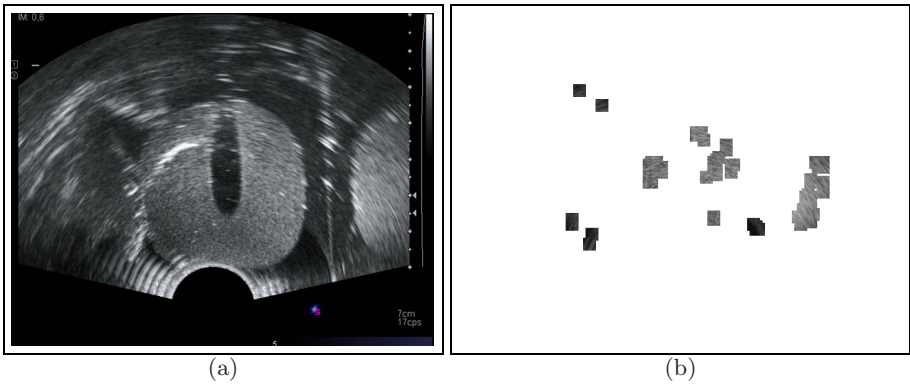


**Fig. 4.** Results in prostatic phantom images. (a) original and (b) speckle detection.

## 4.4 Speckle Detection

Speckle detection results are shown in this section. The algorithm was tested using US images from a prostatic phantom. Although a single image was used for the core speckle detection (more images could be used), detection results are qualitatively satisfactory as shown in Fig. 4. Interestingly, the method detects regions not only with dark speckle patches (similar to the core speckle) but also lighter speckle areas inside the prostate area.

## 5 Conclusion

A novel approach for the detection of speckle in real B-scan images has been presented. We have shown that optimally discriminant speckle statistics can be used for obtaining a better speckle characterisation. In addition, an automatic method for detecting core speckle and non-speckle areas has been presented, which eliminates the need of manual intervention. Quantitative and qualitative results have been given which prove the validity of our approach. Future work will be focused on applying the speckle detection algorithm to particular applications such as 3D reconstruction from sensorless freehand images or increasing signal to noise ratio in US images.

**Acknowledgments.** Work partially supported by MEC grant nbs. TIN2005-08792-C03-01 and TIN2006-08035 and grants from the SERAM and ACMCB.

## References

1. Ghofrani, S., Jahed-Motlagh, M., Ayatollahi, A.: An adaptive speckle suppression filter based on Nakagami distribution. In: IEEE EUROCON'2001, International Conference on Trends in Communications, vol. 1 (2001)
2. Wachowiak, M., Smolikova, R., Zuranda, J., Elmaghraby, A.: Estimation of K distribution parameters using neural networks. *IEEE Transactions on Biomedical Engineering* 49(6), 617–620 (2002)
3. Wagner, R., Smith, S.W., Sandrik, J., Lopez, H.: Statistics of speckle in ultrasound B-scans. *IEEE Transactions on Sonics and Ultrasonics* 30(3), 156–163 (1983)
4. Dutt, V., Greenleaf, J.: Adaptive speckle reduction filter for Log-compressed B-scan images. *IEEE Transactions on Medical Imaging* 15(6), 802–813 (1996)
5. Prager, R., Gee, A., Treece, G., Berman, L.: Speckle Detection in ultrasound images using first order statistics. Technical Report TR 415, University of Cambridge (2001)
6. Dutt, V.: Statistical Analysis of Ultrasound Echo Envelope. PhD thesis, Mayo Graduate School (1995)
7. Martín-Fernández, M., Alberola-López, C.: On low order moments of the Homodyned-K distribution. *Ultrasonics* 43, 283–290 (2005)
8. Webb, A.: Statistical Pattern Recognition, 2nd edn. John Wiley and Sons, New York (2003)